The Astrophysical Journal, 753:13 (8pp), 2012 July 1 doi:10.1088/0004-637X/753/1/13
© 2012. The American Astronomical Society. All rights reserved. Printed in the U.S.A.

A STUDY OF THE ROLE OF Lyβ FLUORESCENCE ON O I LINE STRENGTHS IN Be STARS

Blesson Mathew[1], D. P. K. Banerjee[1], A. Subramaniam[2], and N. M. Ashok[1]
[1] Astronomy and Astrophysics Division, Physical Research Laboratory, Navrangapura, Ahmedabad, Gujarat 380009, India; blesson@prl.res.in
[2] Indian Institute of Astrophysics, Bangalore 560034, India
Received 2011 September 30; accepted 2012 April 25; published 2012 June 8

ABSTRACT

The possibility of the Lyβ fluorescence mechanism being operational in classical Be (CBe) stars and thereby contributing to the strength of the O I λ8446 line has been recognized for long. However, this supposition needs to be quantified by comparing observed and predicted O I line ratios. In the present work, optical and near-infrared spectra of CBe stars are presented. We analyze the observed strengths of the O I λ7774, λ8446, λ11287, and λ13165 lines, which have been theoretically proposed as diagnostics for identifying the excitation mechanism. We have considered and examined the effects of Lyβ fluorescence, collisional excitation, recombination, and continuum fluorescence on these O I line strengths. From our analysis it appears that the Lyβ fluorescence process is indeed operative in Be stars.

Key words: atomic processes – circumstellar matter – infrared: stars – line: formation – stars: emission-line, Be – techniques: spectroscopic

1. INTRODUCTION

Classical Be (CBe) stars are non-supergiant B-type stars whose spectrum, to enable a definition in a broad sense, shows or has shown Balmer lines in emission at some stage (Collins 1987). These and other emission lines are formed in a circumstellar gaseous decretion disk, which is also the source for a significant infrared continuum excess arising from free–free and bound–free emission. It has long been considered that the disk is formed as the outcome of Be stars being fast rotators. However, whether formation of a geometrically thin disk can be caused solely by rotation is not yet a resolved issue (e.g., see the review by Porter & Rivinius 2003). Recent studies suggest that CBe stars are rotating close to their critical velocities and other mechanisms like non-radial pulsations, magnetic fields, or binarity can possibly contribute to explaining the Be phenomenon (Meilland et al. 2012).

The dynamics and nature of the circumstellar disk can be understood better from spectroscopic observations. One of the initial efforts in this direction is by Slettebak (1982) who estimated the spectral types and rotational velocities of 183 Oe-, Be-, and A-F-type shell stars brighter than 6 mag. Subsequently, several other detailed spectroscopic surveys have been done both in the optical (for example Andrillat & Fehrenbach 1982; Andrillat et al. 1988; Dachs et al. 1986; Dachs et al. 1992; Banerjee et al. 2000; Hanuschik 1986; Hanuschik 1987) and in the near-infrared (for example Clark & Steele 2000; Steele & Clark 2001) to understand the behavior and temporal evolution of different lines and in general to understand the Be phenomenon. Our present study focuses on studying the strengths of certain O I lines that are commonly seen in the optical and near-infrared spectra of CBe stars, viz., the O I λ7774, λ8446, λ11287, and λ13165 lines. The motivation for studying these lines is discussed below in greater detail. Our optical sample of CBe stars is drawn from earlier studies by Mathew et al. (2008) and Mathew & Subramaniam (2011) wherein we had surveyed, identified, and obtained spectra of 150 CBe stars in selected open clusters.

Among the O I lines one may begin by considering O I λ8446, which is present in emission in the spectra of several astrophysical sources, viz., emission-line stars, H II regions, planetary nebulae, novae, Seyfert galaxies, and QSOs. It is an interesting line because there has been considerable discussion in the literature on the possible mechanisms that excite it. It is generally accepted that Lyβ fluorescence, apart from other mechanisms like collisional excitation, recombination, and continuum fluorescence, can greatly contribute to the observed strength of the line. The Lyβ fluorescence mechanism was proposed by Bowen (1947) wherein due to the near coincidence of wavelengths, hydrogen Lyβ photons at 1025.72 Å can pump the O I ground state resonance line at 1025.77 Å, thereby populating the O I $3d^3D^0$ level. The subsequent downward cascade produces the λ11287, λ8446, and λ1304 lines in emission. This was referred to as a PAR process (photoexcitation by accidental resonance) by Bhatia & Kastner (1995, hereafter BK95) who constructed a detailed model for neutral oxygen and computed expected strengths of the various O I lines when collisional excitation was the sole excitation mechanism (BK95) and followed it with a second study in which the PAR process was also considered (Kastner & Bhatia 1995, hereafter KB95). In the present study, we have used the results from these two studies to understand the neutral O I spectrum of CBe stars and discriminate whether the PAR process is indeed responsible for the observed strength of the λ8446 line in these stars. That the Lyβ fluorescence process could be operating in CBe stars has long been suggested. For example as early as 1951, Slettebak (1951) in a survey of 25 CBe stars pointed out the anomalies in the strengths of the λ7774 and λ8446 lines with the well-known tendency of λ8446 to go into emission more readily than λ7774. This was attributed to the Lyβ process increasing the strength of the λ8446 line. A similar conclusion was reached by Burbidge (1952) while studying the CBe star χ Oph. However, as of today, observational strengths of the O I lines in Be stars do not appear to have been compared in a comprehensive manner with the detailed theoretical calculations, such as those of BK95 and KB95, to establish whether the Lyβ fluorescence process really affects the neutral O I spectrum. In the present work, we study the behavior of the O I λ7774 and λ8446 lines in the optical and the O I λ11287 and λ13165 lines in the near-infrared and show that there is convincing evidence indicating that the Lyβ fluorescence process is indeed operational in CBe stars.

2. OBSERVATIONS AND ANALYSIS

Our optical sample of CBe stars is drawn from the study of Mathew et al. (2008) who performed a survey to identify CBe stars in 207 open clusters using slitless spectroscopy. The spectroscopy of 150 CBe stars in 39 open clusters in the wavelength range 3800–9000 Å is presented in Mathew & Subramaniam (2011)—the optical spectra analyzed here are from this study. Briefly, these spectroscopic observations were done using the HFOSC imager-spectrograph instrument available on the 2.0 m Himalayan Chandra Telescope, located at Hanle, India. The CCD used for imaging is a 2 K × 4 K CCD, with a pixel size of 15 μm and an image scale of 0.297 arcsec pixel^{-1}. The spectra of CBe stars were taken at an effective resolution of 7 Å around the Hα line. More details on the observations are presented in Mathew & Subramaniam (2011) and details on the HFOSC are available on the Web site at http://www.iiap.res.in. All the observed spectra were wavelength calibrated and corrected for instrument sensitivity using the Image Reduction and Analysis Facility (IRAF) tasks. IRAF was also used for all further data reduction and analysis including measurements of the equivalent widths (W) of the spectral lines—the typical error in the measurement of W values is around 10%.

The J-band spectra were obtained at a resolution of ∼1000 using the Near-Infrared Imager/Spectrometer with a 256 × 256 HgCdTe NICMOS3 array, mounted on the 1.2 m Mt. Abu telescope. For each object a set of two spectra was taken with the star dithered to two different positions along the one-arcsecond-wide slit. Spectral calibration was done using OH airglow and telluric lines, which register with the stellar spectrum. Following the standard practice used in the near-IR, the telluric lines present in the object spectra were removed through a rationing process, in which the object spectrum is divided by the standard star spectrum. The standard star was always observed at a similar airmass as the object and prior to rationing the hydrogen lines in its spectrum were removed by interpolation. The rationed spectra were finally multiplied by a blackbody spectrum, corresponding to the effective temperature of the standard star, to yield the final spectra. The spectra presented here are for the CBe stars HD 10516, HD 12856, HD 19243, HD 35345, β Mon A, and β Mon C, which were observed on 2009 November 8, 2010 December 12, 2009 November 7, 2010 December 13, 2010 October 22, and 2010 October 22, respectively. The corresponding standard stars used were SAO 22696, SAO 22859, SAO 12438, SAO 57819, SAO 151911, and SAO 151911. The spectral data reduction and analysis were done using IRAF tasks. In this work, we have presented the J-band spectra of a few field CBe stars, which have been observed as part of an ongoing program to study the J-band spectra of CBe stars. A detailed analysis of the J-band spectra of CBe stars will be presented later.

3. RESULTS

In the optical, the focus was on studying the strengths of the O I λ7774 and λ8446 lines for reasons outlined below. To study the effects of the H Lyβ/O I PAR process, KB95 concentrated on five visible/infrared lines most relevant to the process. These are the forbidden line at 6300 Å, which serves as a non-fluorescent standard when the line is available, the allowed 8446 Å transition, which is an expected fluorescent product, the allowed multiplet at 7774 Å conventionally thought to be independent of the H Lyβ/O I PAR process, the allowed transition at 11287 Å, which is the primary cascade line in the PAR process, and an additional IR line at 11298 Å. The λ6300 line is a suitable line of choice for examining effects of the PAR process in novae since it is seen in their spectra. However, this line is hardly seen in our CBe spectra except in a few isolated cases where it is extremely weak; it is hence not a suitable diagnostic line for our purpose. On the other hand the λ7774 and λ8846 lines are prominently seen in CBe star spectra and, as emphasized by KB95, their wavelength proximity introduces minimal errors when their strengths are compared even if the line intensities are not deredenned. We have also used the λ11287 and λ13165 near-IR J-band lines since the ratio of their line strengths is an effective discriminator between Lyβ and continuum fluorescence as described in Grandi (1975) and Strittmatter et al. (1977). We note that a comprehensive J-band spectral study of Be stars is unavailable though the H and K bands are well investigated (Clark & Steele 2000; Steele & Clark 2001) as well as the L band (Granada et al. 2010). For that matter, the J-band spectra of even isolated CBe stars are not readily encountered in the literature.

In the present study, CBe stars are broadly classified into three groups based on the nature of O I λ7774 and λ8446 line profiles. Group I comprises of 83 stars which show both the O I λ7774 and λ8446 lines in emission (Figure 1, for a few examples). Out of these 83, 6 stars show the O I lines very weakly in emission, making it difficult to measure the equivalent widths with any accuracy. Therefore we have omitted these stars and considered only 77 stars in Group I for the present analysis. Group II show O I λ8446 in emission and λ7774 in absorption with 26 CBe stars belonging to this category (top panel of Figure 2). Group III mostly includes objects (23 CBe stars) in which O I λ8446 is in emission but λ7774 is not prominent enough for a clear-cut classification, with the spectra we have, into an absorption or emission group (bottom panel of Figure 2). For comparing strengths of the λ7774 and λ8446 lines, it is meaningful to use only objects where both lines are in emission; we have thus restricted the analysis described below to objects from the first group.

3.1. Correction for Measured O I Equivalent Widths

To estimate the equivalent width of O I λ8446, it is necessary to deblend this line from Paschen 18 (P18, 8437 Å). It is possible to estimate the value of W(P18) by linearly interpolating between measured equivalent widths of the flanking lines P17 (8467 Å) and P19 (8413 Å) since the emission monotonically decreases along the Paschen series in this region as indicated by Briot (1981a) and Briot (1981b). This value of W(P18) may then be subtracted from the combined equivalent width of W(8446 + P18) to get the intrinsic value of W(8446) in emission. To confirm the validity of this procedure we have plotted in Figure 3 the ratio of the mean equivalent widths of P14, P17, P19, P20, P21 normalized to the equivalent width of P17. In this figure, we do not include P15 and P16 because they are blended with the Ca II lines at 8542 and 8498 Å. The mean equivalent widths of the Paschen lines were computed from a sample of 26 stars, which best showed these lines and at a good signal-to-noise ratio. Such a selection enables us to measure the equivalent widths of these lines in a manner which is most reliable. The expected position of P18 (8437 Å) is shown by a dashed line. As may be seen from Figure 3, the Paschen line strengths do show a monotonical increase with wavelength and then display a trend of flattening out around P17 and beyond. For our purpose of estimating the equivalent width of P18 it looks reasonable from the figure to

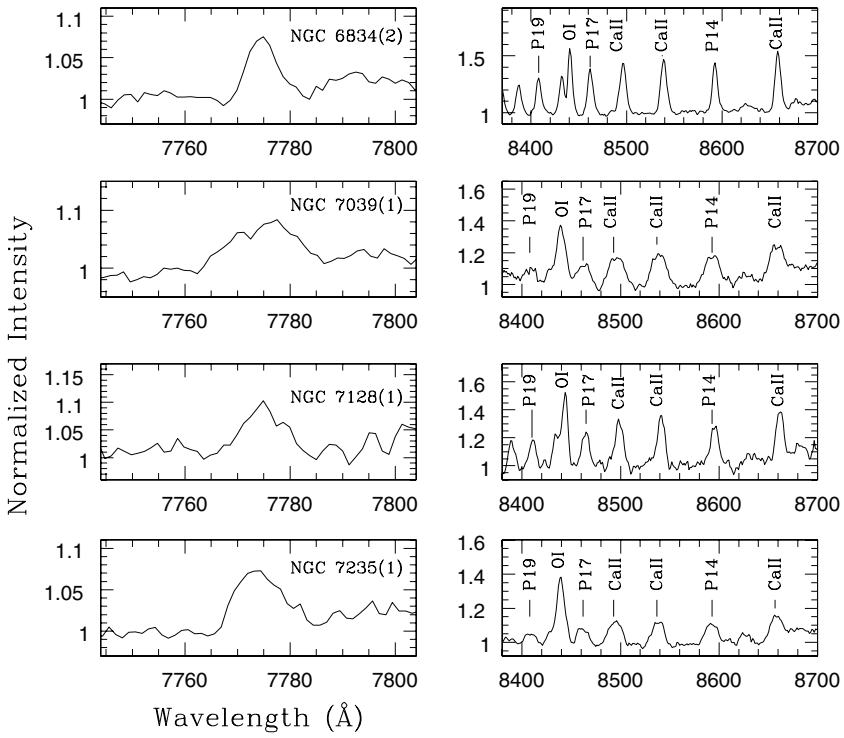

Figure 1. O I λ7774 and λ8446 line profiles of Group I candidates NGC 6834(2), NGC 7039(1), NGC 7128(1), and NGC 7235(1). Along with O I λ8446 which is blended with hydrogen Paschen 18 (P18), other lines seen are P14 λ8598, P17 λ8467, P19 λ8413, and Ca II λ8498, λ8542, λ8662. The nomenclature of these CBe stars is given in Mathew & Subramaniam (2011).

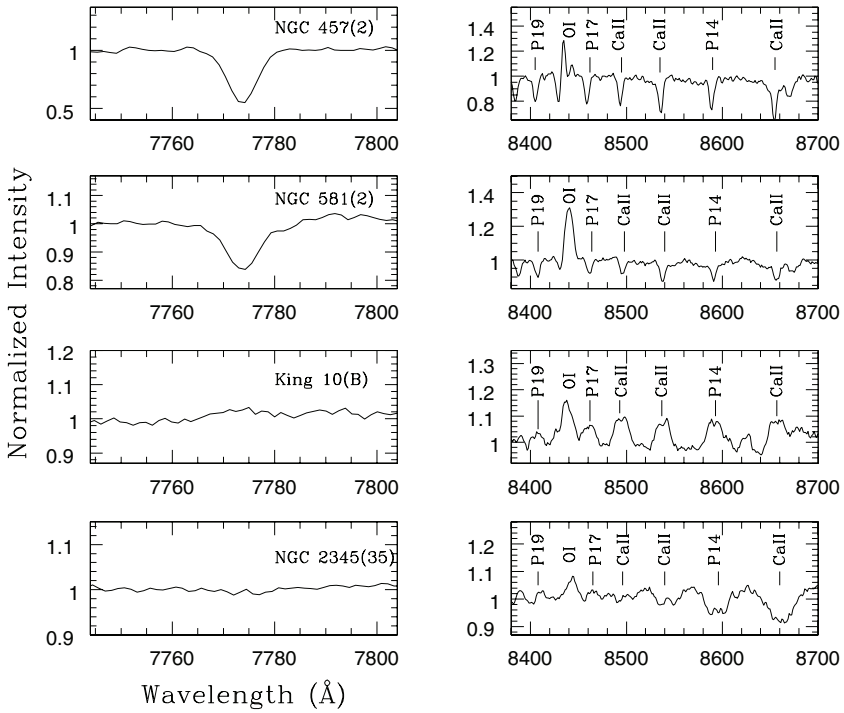

Figure 2. O I λ7774 and λ8446 line profiles of Group II candidates (1) NGC 457(2), (2) NGC 581(2) are shown in the upper panel while that of Group III candidates (3) King 10(B), (4) NGC 2345(35) are shown in the lower panel.

approximate the value by interpolating between the equivalent width values of P17 and P19, individually for each star.

The flattening behavior of the Paschen line strengths beyond P17, shown in Figure 3, is possibly because these lines are optically thick and therefore being seen at a reduced intensity compared to that expected from recombination Case B analysis (Hummer & Storey 1987; Storey & Hummer 1995). Similar behavior is seen for Brackett series lines (Steele & Clark 2001) and Humphrey and Pfund lines (Granada et al. 2010), which is attributed to optical depth effects.

Subsequent to the correction of $W(8446)$ from the contribution of P18, $W(7774)$ and $W(8446)$ are corrected for the

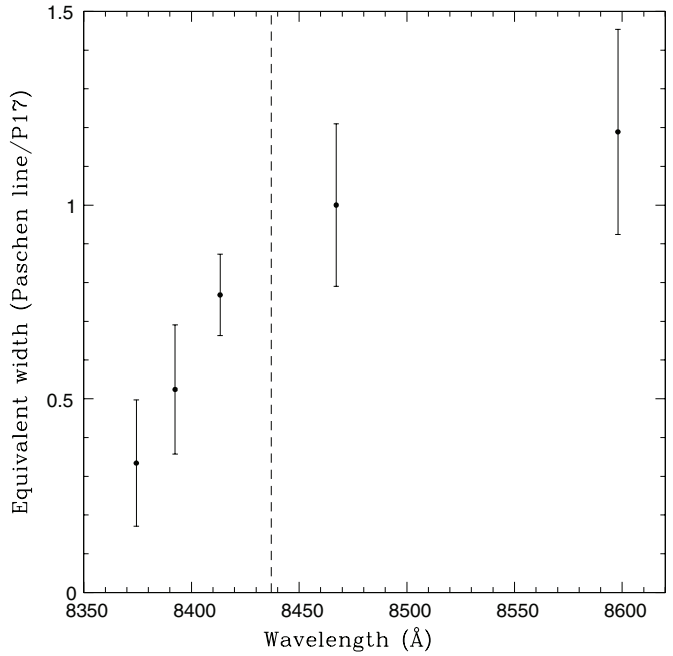

Figure 3. Ratio of the mean equivalent widths of the unblended Paschen lines P14, P17, P19, P20, and P21 normalized to the equivalent width of P17. The corresponding wavelengths of these lines are 8598, 8467, 8413, 8392, and 8374 Å, respectively. The wavelength position of P18 (8437 Å) is shown in dashed line. Further details are given in the text in Section 3.1.

underlying stellar absorption. This is necessary because these lines come into emission only after filling the underlying absorption component. The strength of this absorption component is estimated from the synthetic spectra of B0–B9 main-sequence stars of solar metallicity given by Munari et al. (2005), which are calculated from the SYNTHE code (Kurucz 1993) using NOVER models as the input stellar atmospheres (Castelli et al. 1997). We find W values of the components for the B0–B9 classes, respectively, to be 0.006, 0.099, 0.143, 0.178, 0.209, 0.248, 0.272, 0.304, 0.345, and 0.400 Å, respectively, for the λ7774 line and 0.003, 0.050, 0.074, 0.095, 0.111, 0.136, 0.153, 0.173, 0.199, and 0.236 for the λ8446 line. These equivalent width values of the λ7774 and λ8446 absorption components are added to their corresponding emission values measured from the observed spectra to yield the final W values of the lines. The ratio of these equivalent widths is converted into a flux ratio by multiplying it with the ratio of continuum fluxes at 7774 and 8446 Å, which is obtained from Kurucz (1992) models which are also given by Leitherer (http://www.stsci.edu/science/starburst/Kurucz.html). Typically the 7774/8446 continuum ratios from the Kurucz models are in the range 1.34–1.26 for B0–B9 and closely match the 7774/8446 continuum ratio expected of a blackbody having an effective temperature of the corresponding B-type star's spectral class.

The derived line flux ratio is finally corrected for extinction where the extinction at 7774 and 8446 Å is derived from the parameterized, seventh-order polynomial fit to the interstellar extinction given in Cardelli et al. (1989). This gives $A(7774) = 0.6307A_V$ and $A(8446) = 0.5275A_V$ or equivalently $A(7774)$–$A(8446) = 0.32 \times E(B-V)$ with a ratio of total-to-selective extinction of $R = 3.1$. The $E(B-V)$ values of the CBe stars are assumed to be equal to the mean $E(B-V)$ of the cluster with which it is associated. These values, available from the literature, are compiled in Mathew et al. (2008) and were used for extinction correction and are shown in Column 9 of Table 1. However, it may be noted that the circumstellar envelope of a CBe star itself introduces an additional reddening expected to be of the order of $E(B-V) \sim 0.1$ mag (Dachs et al. 1988; Slettebak 1985). But this component is small compared to the cluster reddening (Column 9, Table 1) and therefore should not significantly affect the dereddening corrections to the O I line flux ratio. The final deredenned line flux ratio $I(8446/7774)$, using the cluster $E(B-V)$ value, is given in Column 10 of Table 1 and plotted in the right-hand panel of Figure 4. In the case which we include the 0.1 mag additional reddening due to the circumstellar envelope, the $I(8446/7774)$ ratio is found to change very marginally by ∼3%.

3.2. Possibility of PAR Process as the Dominant Excitation Mechanism for O I Emission Lines in CBe Stars

The expected $I(8446/7774)$ ratio from KB95, in the absence of the PAR process (i.e., the parameter $R_p = -\infty$), is shown in Figure 4 (right-hand panel) as straight lines. Essentially $R_p = -\infty$ represents the case of pure collisional excitation considered by BK95. The $I(8446/7774)$ ratio is shown at two temperatures of 10,000 K and 20,000 K and three values of the electron density $n_e = 10^{10}$, 10^{11}, and 10^{12} cm^{-3}. The choice of this parameter space for n_e and T is a realistic approximation of the actual range over which these parameters vary in the Be star disk. There are several studies available in the literature that model Be star disks in great detail to estimate disk parameters (e.g., Sigut & Jones 2007; Carciofi & Bjorkman 2008; Gies et al. 2007). We find that a global view of disk parameters is offered by the work of Silaj et al. (2010) who generate and compare the model and observed emission profiles for a statistically large sample of 57 CBe stars. These models use the code of Sigut & Jones (2007). The current models mentioned above assume that the disk density decreases, starting from a base density value of ρ_0, with radial distance R as a power law with exponent n (that is, $\rho \propto \rho_0(R_{\rm star}/R)^n$). Silaj et al. (2010) point out that one of the interesting features of the derived disk density parameters is that a radial power-law index of $n = 3.5$ is strongly preferred for the model fits with 43% of the fits, over all stars considered, requiring this power-law index. We adopt this as a representative value for n. From their individually listed values of ρ_0 for the entire sample, we find a mean value of 1.09×10^{-10} gm cm^{-3} for ρ_0 equivalent to a density of 6.5×10^{13} electrons cm^{-3}, assuming a completely ionized gas composed purely of hydrogen. With $n = 3.5$ and a mean value of ρ_0 as above, and assuming a mean disk size of 6–8 $R_{\rm star}$, the density ranges from 6.5×10^{13} at the inner edge to ∼(0.5 to 1.2) $\times$ 10^{11} electrons cm^{-3} at the outer edge of the disk. Thus, a mean or representative value of n_e across the disk should be taken as 1×10^{11} cm^{-3} or greater; this is what we will adopt. The above models also show that the disk is not isothermal but the temperature of the matter in the disk is mostly seen to be in the range of 10,000–20,000 K.

Figure 4 (right panel) shows that for the adopted values of $n_e = 1 \times 10^{11}$ cm^{-3} and $T = 10{,}000$ to 20,000 K, the $I(8446/7774)$ ratio of all stars barring one lies above the value predicted from pure collisional excitation. This is also true for the case of $n_e = 10^{12}$ cm^{-3} and, from the trend, should be true for higher densities too. The expected value of $I(8446/7774)$ for $n_e = 10^{10}$ cm^{-3} is also shown, more to illustrate the dependence on n_e and T, but as argued before this is likely a lower than actual value for the electron density. Even in this case, a large number of stars show $I(8446/7774)$ to

Table 1
List of CBe Stars which Show O I λ7774 and λ8446 in Emission Shown with Equivalent Width and Line Flux Ratio Estimates

Be Star	Sp. Type	Obs. Date	$W(7774)^a$	$W(8446)^a$	$W(7774)^b$	$W(8446)^b$	$I(8446/7774)$	$E(B-V)$	$I_C{}^c$
Berkeley86(26)	B1V	2005 Jun 27	−0.31	−1.72	−0.41	−1.77	3.22	0.90	2.47
Berkeley87(3)	B2	2005 Oct 8	−0.41	−0.45	−0.55	−0.52	0.71	1.90	0.41
Berkeley87(4)	B0-1V	2005 Oct 9	−0.45	−3.29	−0.50	−3.31	4.98	1.53	3.17
Berkeley90(1)	B0V	2006 Agu 28	−0.76	−3.77	−0.77	−3.77	3.68	1.15	2.62
Collinder96(1)	B0-1V	2005 Nov 21	−0.36	−1.81	−0.41	−1.84	3.37	0.48	2.93
IC4996(1)	B3	2005 Jul 15	−0.10	−1.44	−0.28	−1.53	4.23	0.71	3.43
King10(A)	B1V	2005 Jul 29	−0.50	−1.58	−0.60	−1.63	2.03	1.13	1.45
King10(C)	B2V	2005 Jul 30	−0.16	−0.54	−0.30	−0.61	1.54	1.13	1.10
King10(E)	B3V	2005 Jul 31	−0.12	−1.38	−0.30	−1.47	3.81	1.13	2.73
NGC436(2)	B5-7V	2007 Jan 10	−0.96	−1.44	−1.23	−1.59	1.03	0.50	0.89
NGC436(5)	B3V	2007 Jan 9	−0.42	−1.72	−0.60	−1.81	2.34	0.50	2.02
NGC457(1)	B3V	2006 Sep 29	−0.08	−1.05	−0.26	−1.14	3.41	0.49	2.95
NGC581(1)	B2V	2006 Sep 28	−0.46	−1.63	−0.60	−1.70	2.15	0.44	1.89
NGC581(3)	B0-1V	2006 Sep 28	−0.30	−1.18	−0.35	−1.20	2.58	0.44	2.27
NGC654(2)	B0-1	2006 Sep 29	−1.01	−3.08	−1.06	−3.10	2.20	0.90	1.69
NGC659(1)	B2V	2005 Nov 21	−0.53	−2.30	−0.67	−2.37	2.68	0.63	2.23
NGC659(3)	B1V	2005 Nov 21	−0.40	−0.70	−0.50	−0.75	1.12	0.63	0.93
NGC663(1)	B5V	2005 Oct 8	−0.70	−1.64	−0.95	−1.78	1.43	0.80	1.13
NGC663(2)	B0-1V	2005 Oct 7	−0.39	−2.63	−0.44	−2.66	4.54	0.80	3.59
NGC663(4)	B1V	2005 Oct 24	−0.38	−1.57	−0.48	−1.62	2.51	0.80	1.98
NGC663(5)	B1V	2005 Nov 22	−1.34	−3.14	−1.44	−3.19	1.65	0.80	1.30
NGC663(9)	B1V	2005 Oct 24	−1.11	−4.17	−1.21	−4.22	2.60	0.80	2.05
NGC663(11)	B2V	2005 Oct 9	−0.42	−2.18	−0.56	−2.25	3.04	0.80	2.40
NGC663(12V)	B0-1V	2005 Nov 21	−0.27	−3.07	−0.32	−3.10	7.27	0.80	5.74
NGC663(15)	B1V	2005 Oct 25	−0.80	−2.05	−0.90	−2.10	1.74	0.80	1.37
NGC663(16)	B1V	2005 Oct 25	−0.55	−1.65	−0.65	−1.70	1.95	0.80	1.54
NGC663(P5)	B2V	2005 Oct 14	−0.64	−2.31	−0.78	−2.38	2.31	0.80	1.82
NGC663(P8)	B2V	2005 Oct 14	−0.32	−1.45	−0.46	−1.52	2.51	0.80	1.98
NGC663(P23)	B2V	2005 Oct 25	−0.28	−1.08	−0.42	−1.15	2.08	0.80	1.64
NGC663(P25)	B0-1V	2005 Nov 22	−0.15	−0.61	−0.20	−0.64	2.41	0.80	1.90
NGC869(1)	B0V	2006 Jan 21	−0.92	−5.23	−0.93	−5.23	4.23	0.56	3.59
NGC869(2)	B0-1V	2006 Jan 20	−0.56	−1.16	−0.61	−1.18	1.45	0.56	1.23
NGC869(5)	B1V	2006 Jan 20	−0.32	−1.00	−0.42	−1.05	1.86	0.56	1.58
NGC884(1)	B0-1V	2006 Jan 22	−0.71	−0.83	−0.76	−0.86	0.84	0.56	0.71
NGC884(2)	B0-1V	2006 Jan 22	−1.06	−5.50	−1.11	−5.53	3.74	0.56	3.17
NGC884(5)	B0V	2006 Sep 28	−0.56	−1.52	−0.57	−1.52	2.00	0.56	1.70
NGC957(1)	B0-1V	2005 Dec 7	−0.67	−3.26	−0.72	−3.28	3.43	0.84	2.68
NGC1220(1)	B5V	2005 Nov 21	−0.87	−2.34	−1.12	−2.48	1.68	0.70	1.37
NGC1893(1)	B1V	2005 Nov 21	−1.22	−5.14	−1.32	−5.19	2.93	0.58	2.47
NGC2345(27)	B3V	2007 Dec 28	−1.01	−2.10	−1.19	−2.19	1.43	0.77	1.14
NGC2345(59)	B3V	2005 Dec 7	−0.82	−1.55	−1.00	−1.64	1.27	0.54	1.08
NGC2345(X2)	B5V	2007 Dec 15	−0.57	−1.89	−0.82	−2.03	1.88	0.50	1.62
NGC2414(2)	B1V	2005 Dec 7	−0.23	−1.69	−0.33	−1.74	3.93	0.51	3.38
NGC2421(1)	B1V	2006 Jan 21	−0.69	−3.22	−0.79	−3.27	3.09	0.42	2.73
NGC6649(1)	B0V	2007 Jun 9	−0.70	−2.69	−0.71	−2.69	2.84	1.20	1.99
NGC6649(6)	B5V	2007 Jun 10	−0.55	−1.84	−0.80	−1.97	1.88	1.20	1.32
NGC6649(7)	B2V	2007 Jun 10	−0.84	−3.55	−0.98	−3.62	2.80	1.20	1.97
NGC6834(1)	B5V	2005 Oct 7	−1.11	−3.10	−1.36	−3.23	1.81	0.61	1.51
NGC6834(2)	B1V	2005 Oct 7	−0.49	−2.85	−0.59	−2.90	3.67	0.61	3.07
NGC7039(1)	B1-3V	2005 Nov 21	−1.14	−1.99	−1.28	−2.06	1.22	0.19	1.15
NGC7128(1)	B1V	2005 Oct 14	−0.88	−3.57	−0.98	−3.62	2.76	1.03	2.04
NGC7235(1)	B0-1V	2005 Oct 14	−0.75	−3.51	−0.80	−3.53	3.32	0.90	2.55
NGC7261(1)	B0V	2005 Dec 7	−1.03	−3.90	−1.04	−3.90	2.82	0.97	2.12
NGC7261(2)	B1V	2005 Dec 7	−0.26	−0.67	−0.36	−0.72	1.49	0.97	1.12
NGC7261(3)	B0-1V	2005 Dec 7	−0.73	−2.65	−0.78	−2.67	2.57	0.97	1.93
NGC7380(2)	B1-3V	2006 Jul 17	−0.73	−2.83	−0.87	−2.90	2.53	0.60	2.12
NGC7380(3)	B1-3V	2006 Jul 17	−0.47	−1.63	−0.61	−1.70	2.11	0.60	1.77
NGC7419(A)	B0V	2005 Jul 15	−0.43	−3.34	−0.44	−3.34	5.70	1.65	3.50
NGC7419(B)	B0V	2005 Jun 27	−0.92	−3.55	−0.93	−3.55	2.87	1.65	1.76
NGC7419(D)	B1V	2005 Jul 15	−1.28	−4.20	−1.38	−4.25	2.30	1.65	1.41
NGC7419(E)	B6	2005 Jul 31	−1.13	−6.24	−1.40	−6.39	3.62	1.65	2.23
NGC7419(G)	B0V	2005 Agu 8	−1.10	−4.35	−1.11	−4.35	2.95	1.65	1.81
NGC7419(I)	B0V	2005 Jul 15	−0.60	−2.77	−0.61	−2.77	3.41	1.65	2.10
NGC7419(J)	B0V	2005 Agu 8	−0.25	−0.72	−0.26	−0.72	2.08	1.65	1.28
NGC7419(L)	B0V	2005 Jul 15	−0.73	−3.61	−0.74	−3.61	3.67	1.65	2.26
NGC7419(M)	B0V	2005 Agu 8	−0.37	−2.54	−0.38	−2.54	5.02	1.65	3.09

Table 1
(Continued)

Be Star	Sp. Type	Obs. Date	$W(7774)^a$	$W(8446)^a$	$W(7774)^b$	$W(8446)^b$	$I(8446/7774)$	$E(B-V)$	$I_C{}^c$
NGC7419(N)	B2.5	2005 Agu 8	−1.41	−7.39	−1.57	−7.47	3.66	1.65	2.25
NGC7419(O)	B8V	2005 Agu 8	−0.68	−2.29	−1.02	−2.49	1.94	1.65	1.19
NGC7419(Q)	B1-3V	2005 Agu 8	−1.21	−7.57	−1.35	−7.64	4.29	1.65	2.64
NGC7419(1)	B0V	2005 Oct 7	−0.94	−4.77	−0.95	−4.77	3.77	1.65	2.32
NGC7419(3)	B0V	2005 Agu 8	−1.51	−6.81	−1.52	−6.81	3.37	1.65	2.07
NGC7419(4)	B0V	2005 Oct 7	−0.16	−2.39	−0.17	−2.39	10.6	1.65	6.52
NGC7419(5)	B0V	2005 Oct 7	−1.09	−6.13	−1.10	−6.13	4.19	1.65	2.58
NGC7510(1A)	B0V	2005 Oct 24	−0.56	−3.50	−0.57	−3.50	4.62	1.12	3.32
NGC7510(1B)	B1V	2005 Oct 12	−0.69	−1.36	−0.79	−1.41	1.33	1.12	0.96
NGC7510(1C)	B0V	2005 Oct 13	−0.92	−5.27	−0.93	−5.27	4.26	1.12	3.06
Roslund4(2)	B0V	2005 Oct 25	−0.68	−6.17	−0.69	−6.17	6.72	1.10	4.86

Notes. The coordinates and details of CBe stars are given in Mathew & Subramaniam (2011).
[a] Observed equivalent widths in Å.
[b] Equivalent widths in Å corrected for underlying stellar absorption component.
[c] This column gives the extinction-corrected line flux ratio of $I(8446/7774)$.

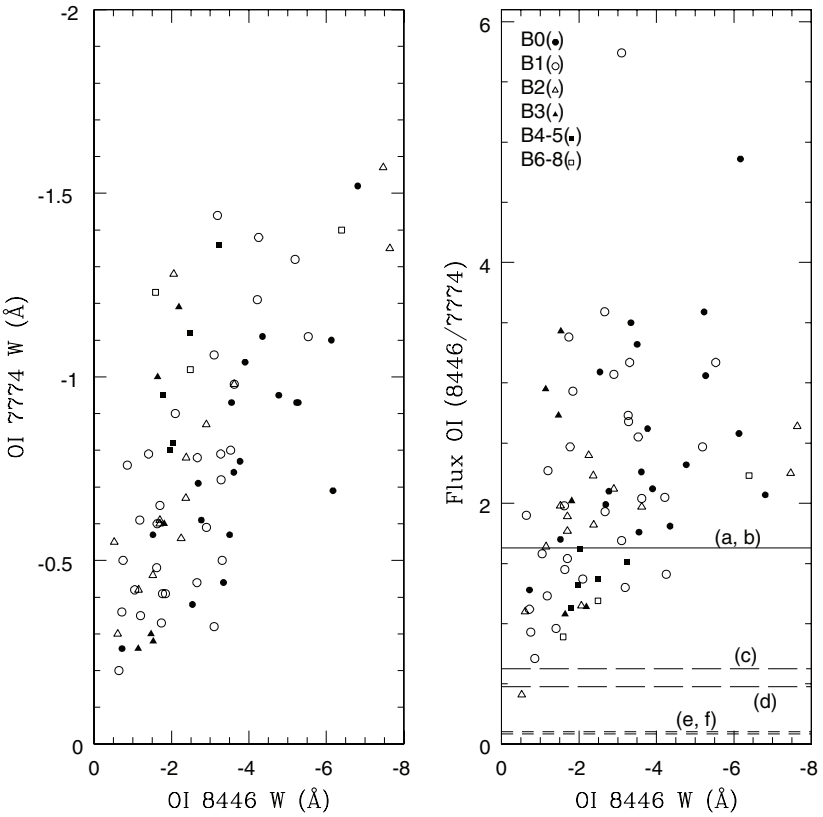

Figure 4. Plot between equivalent widths of the λ7774 and λ8446 lines for the sample of CBe stars is shown in the left panel. The flux ratio $I(8446/7774)$ is shown in the right panel. Horizontal lines indicate the expected values of $I(8446/7774)$, from KB95, in the case of pure collisional excitation. The values are (a) 1.62 for $T =$ 10,000 K, $n_e = 10^{10}$ cm^{-3}; (b) 1.63 for $T = 20{,}000$ K, $n_e = 10^{10}$ cm^{-3}; (c) 0.626 for $T = 10{,}000$ K, $n_e = 10^{11}$ cm^{-3}; (d) 0.478 for $T = 20{,}000$ K, $n_e = 10^{11}$ cm^{-3}; (e) 0.102 for $T = 10{,}000$ K, $n_e = 10^{12}$ cm^{-3}; and (f) 0.083 for $T = 20{,}000$ K, $n_e = 10^{12}$ cm^{-3}. The stars are binned based on their spectral types; B0: filled circles; B1: open circles; B2: open triangles; B3: filled triangles; B4–B5: filled squares; and B6–B8: open squares.

be significantly larger than expected. This shows that collisional excitation by itself cannot account for the higher-than-expected $I(8446/7774)$ ratio observed in Be stars and the PAR process, which enhances the strength of O I λ8446, also contributes. In contrast, it may be mentioned that in the solar chromosphere $I(8446/7774)$ is found to be equal to 0.2 ± 0.02 by Penn (1999) who therefore concludes that collisional excitation is more important than the PAR process in O I solar limb emission.

In Figure 4, the $I(8446/7774)$ strengths at densities of $n_e = 10^{10}$ and 10^{12} are from KB95. But since they have listed their data for increments in $\log n_e$ in steps of 2 (i.e., $\log n_e =$ 4, 6, 8, 10, and 12), the value of $I(8446/7774)$ at other intermediate densities such as $n_e = 10^9, 10^{11}$, etc., was obtained from the authors by writing to them (A. K. Bhatia 2006, private communication).

Although the density exponent $n = 3.5$ is favored by the Silaj et al. (2010) models, other values of the exponent could be considered too. But it may be noted that the bulk of their profiles, 84% to be precise, are modeled with $n \leqslant 3.5$. If we thus consider lower values of n, the density decline in the

disk will be even slower compared to the $n = 3.5$ case. This will strengthen support for our arguments to consider a mean density in the disk of 10^{11} or more. An additional consideration may also be taken into account. Though interferometric data are now gradually emerging on the emission zone size of lines like Hα (e.g., Quirrenbach et al. 1997) and a few other near-IR lines (e.g., Gies et al. 2007; Millan-Gabet et al. 2010), no measurements are yet reported for the size of the O I line emitting region. But indirect estimates about the sizes of line emitting regions have been reported by Jaschek & Jaschek (1993) based on the observed velocity separation of the V (violet) and R (red) components of Be line profiles and the model by Huang (1972). Based on the entire Jaschek data, we have derived the O I λ8446 line emission region to have a mean size of 0.71 ± 0.27 of the Hα emission region size. This implies that O I emission arises from relatively inner regions of the disk and therefore regions of higher density. Following Jaschek & Jaschek (1993), we estimate the radius of the Hα emission region for the 10 CBe stars that showed double-peaked Hα emission line profiles from the sample studied by Mathew & Subramaniam (2011). The mean value is around 12 R_s and 3.5 R_s for Keplerian and rigid body rotation for the particles in the disk. This translates to 8.5 R_s and 2.9 R_s for the size of the O I λ8446 emission region since the O I λ8446 line emission region is 0.71 times the Hα emission radius, as derived earlier.

In Figure 4, we have also indicated the spectral class of the stars. Visual examination does not appear to indicate any significant correlation between the O I ratio and the spectral class. It may be expected that the temperature of the central star, which is essentially a measure of the spectral class, could affect the strength of the O I λ8446 line via the amount of Lyβ radiation that the star emits. Even though this result looks promising, it needs to be strengthened further from the analysis of a large sample of CBe stars, especially late-type CBe stars.

If Lyβ fluorescence is operational in CBe stars one would expect a correlation between the emission strength of Hα and O I λ8446 lines, since Hα and Lyβ both depend on the population of the third hydrogen level (Bowen 1947). Kitchin & Meadows (1970) and Andrillat et al. (1988) have studied the correlation between the measured equivalent widths of Hα and O I λ8446 emission lines in CBe stars. With our simultaneous observations of O I λ8446 and Hα, it is interesting to derive a relation between their emission line equivalent widths. The W(Hα) values for this analysis are for the same sample of stars analyzed here but whose equivalent width values are reported in Mathew & Subramaniam (2011) while W(8446) values are given in Table 1. From a simple linear fit, we have derived the following relation between W(Hα) and W(8446), both measured in Å, for Group I stars as

$$W(8446) = 0.10 \times W(H\alpha) + 0.53. \quad (1)$$

It is unlikely that recombination plays a dominant role in O I excitation since the I(8446/7774) ratio, in the case of recombination, should be around 0.6 as indicated by Grandi (1975, 1980) and Strittmatter et al. (1977). However, this is not the case here with the λ8446 line being stronger than the λ7774 line in most cases, contrary to expectations. An interesting example where the I(8446/7774) ratio becomes large due to the absence of recombination is in the Weigelt blobs around the LBV η Carinae. As proposed by Johansson & Letokhov (2005), the front of the blobs is ionized providing the Lyβ flux for the PAR process while the inner and distal regions of the blobs remain neutral because the ionizing flux cannot penetrate deep into the blobs. As a result recombination does not occur while

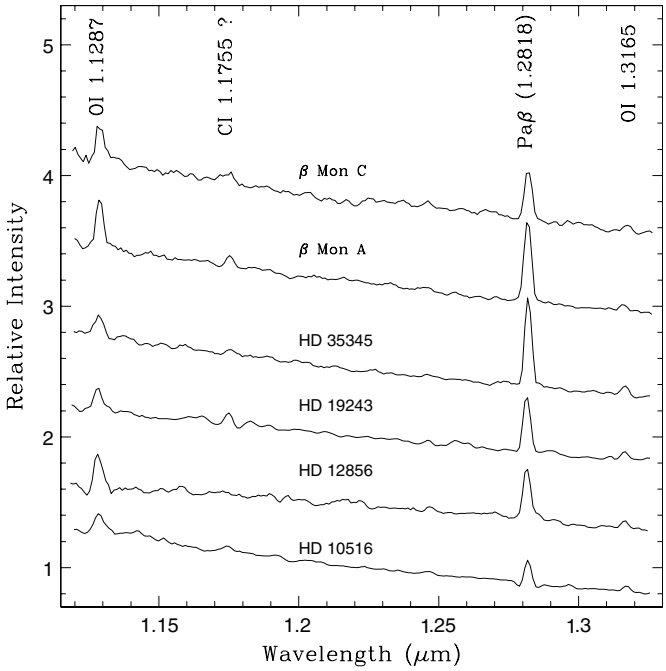

Figure 5. J-band spectra of selected CBe stars with the prominent lines identified. The spectra of the stars HD 10516, HD 12856, HD 19243, HD 35345, β Mon A, β Mon C are normalized with respect to the band center at 1.22 μm. There is an offset between the adjacent spectra for clarity.

the PAR process dominates leading to the extreme case of strong λ8446 emission being seen while the λ7774 line is completely absent.

Whether continuum fluorescence is the main source of excitation or not can be strongly constrained based on the ratio of strengths of the near-IR λ11287 and λ13165 lines. It is expected that $W(13165)/W(11287) \geqslant 1$ if continuum fluorescence is the significant excitation mechanism (Strittmatter et al. 1977; Grandi 1975). On the other hand, if the Lyβ fluorescence process dominates, the λ11287 line should become very strong as it is the primary line of the fluorescent cascade. The $W(13165)/W(11287)$ ratio is then expected to reverse and become smaller than unity. In novae, a large number of which have been studied by us in the near-IR (e.g., nova V1280 Sco, Das et al. 2008; nova V574 Puppis, Naik et al. 2010), it is inevitably seen that $W(11287)$ is several times larger than $W(13165)$, strongly supporting the dominance of the PAR process in novae—analysis of other optical O I lines independently establishes this (KB 95). An extreme case of a nova with extremely strong emission in the λ11287 line accompanied by no emission at 11365 Å is V4643 Sgr (Ashok et al. 2006); nova V1500 Cygni also shows similar and extremely strong fluorescent lines of O I (Strittmatter et al. 1977).

In Figure 5, we present the J-band spectra of selected CBe stars from a larger sample studied by us to characterize their J-band behavior (paper in preparation). It is found that whenever the λ11287 and λ13165 lines are present, as in the spectra shown, the former is always stronger of the two. This is seen in the spectra of Figure 5 where a mean value of $W(13165)/W(11287) = 0.30$ is found. Collisional excitation is also predicted to give $W(13165)/W(11287) \geqslant 1$ at $T = 10{,}000$ and 20,000 K, respectively, for $n_e = 10^{10}$–10^{12} cm^{-3} (BK95). Thus, both continuum fluorescence and collisional excitation are expected to make the λ13165 line stronger than λ11287 line. This is not seen and the $W(13165)/W(11287)$ ratio thus suggests that the Lyβ process

has a significant role in exciting the near-IR lines in CBe stars. It may also be noted that continuum fluorescence if present is expected to give significant contribution to the O I λ7254 and λ7002 lines (Strittmatter et al. 1977) and so also strong emission, comparable to O I λ8446 in the O I λ7990 line (Netzer & Penston 1976). No traces of these O I lines are seen in our spectra within the detection limits (Mathew & Subramaniam 2011). Based on the above evidence and arguments in favor of the PAR process vis-a-vis other excitation mechanisms, we would conclude that the Lyβ fluorescence is operational in CBe stars.

We thank the referee for his suggestions and comments which helped improve the manuscript. One of us (D.P.K.B.) thanks Dr. A. K. Bhatia for his help in providing additional computational data to us. The research work at Physical Research Laboratory is funded by the Department of Space, Government of India.

REFERENCES

Andrillat, Y., & Fehrenbach, Ch. 1982, A&AS, 48, 93
Andrillat, Y., Jaschek, M., & Jaschek, C. 1988, A&AS, 72, 129
Ashok, N. M., Banerjee, D. P. K., Varricatt, W. P., & Kamath, U. S. 2006, MNRAS, 368, 592
Banerjee, D. P. K., Rawat, S. D., & Janardhan, P. 2000, A&AS, 147, 229
Bhatia, A. K., & Kastner, S. O. 1995, ApJS, 96, 325
Bowen, I. S. 1947, PASP, 59, 196
Briot, D. 1981a, A&A, 103, 1
Briot, D. 1981b, A&A, 103, 5
Burbidge, E. M. 1952, ApJ, 115, 418
Carciofi, A. C., & Bjorkman, J. E. 2008, ApJ, 684, 1374
Cardelli, J. A., Clayton, G. C., & Mathis, J. S. 1989, ApJ, 345, 245
Castelli, F., Gratton, R. G., & Kurucz, R. L. 1997, A&A, 318, 841
Clark, J. S., & Steele, I. A. 2000, A&AS, 141, 65
Collins, G. W. 1987, in IAU Colloq. 92, Physics of Be Stars, ed. A. Slettebak & T. P. Snow (Cambridge: Cambridge Univ. Press), 3
Dachs, J., Hanuschik, R., Kaiser, D., Ballereau, D., & Bouchet, P. 1986, A&AS, 63, 87
Dachs, J., Hummel, W., & Hanuschik, R. W. 1992, A&AS, 95, 437
Dachs, J., Kiehling, R., & Engels, D. 1988, A&A, 194, 167
Das, R. K., Banerjee, D. P. K., Ashok, N. M., & Chesneau, O. 2008, MNRAS, 391, 1874
Gies, D. R., Bagnuolo, W. G., Jr., Baines, E. K., et al. 2007, ApJ, 654, 527
Granada, A., Arias, M. L., & Cidale, L. S. 2010, AJ, 139, 1983
Grandi, S. A. 1975, ApJ, 196, 465
Grandi, S. A. 1980, ApJ, 238, 10
Hanuschik, R. W. 1986, A&A, 166, 185
Hanuschik, R. W. 1987, A&A, 173, 299
Huang, S.-S. 1972, ApJ, 171, 549
Hummer, D. G., & Storey, P. J. 1987, MNRAS, 224, 801
Jaschek, C., & Jaschek, M. 1993, A&AS, 97, 807
Johansson, S., & Letokhov, V. S. 2005, MNRAS, 364, 731
Kastner, S. O., & Bhatia, A. K. 1995, ApJ, 439, 346
Kitchin, C. R., & Meadows, A. J. 1970, Ap&SS, 8, 463
Kurucz, R. 1993, SYNTHE Spectrum Synthesis Programs and Line Data, CD-ROM No. 18
Kurucz, R. L. 1992, in IAU Symp. 149, The Stellar Populations of Galaxies, ed. B. Barbuy & A. Renzini (Cambridge: Cambridge Univ. Press), 225
Mathew, B., & Subramaniam, A. 2011, Bull. Astron. Soc. India, 39, 517
Mathew, B., Subramaniam, A., & Bhatt, B. C. 2008, MNRAS, 388, 1879
Meilland, A., Millour, F., Kanaan, S., et al. 2012, A&A, 538, A110
Millan-Gabet, R., Monnier, J. D., Touhami, Y., et al. 2010, ApJ, 723, 544
Munari, U., Sordo, R., Castelli, F., & Zwitter, T. 2005, A&A, 442, 1127
Naik, S., Banerjee, D. P. K., Ashok, N. M., & Das, R. K. 2010, MNRAS, 404, 367
Netzer, H., & Penston, M. V. 1976, MNRAS, 174, 319
Penn, M. J. 1999, ApJ, 518, L131
Porter, J. M., & Rivinius, T. 2003, PASP, 115, 1153
Quirrenbach, A., Bjorkman, K. S., Bjorkman, J. E., et al. 1997, ApJ, 479, 477
Sigut, T. A. A., & Jones, C. E. 2007, ApJ, 668, 481
Silaj, J., Jones, C. E., Tycner, C., Sigut, T. A. A., & Smith, A. D. 2010, ApJS, 187, 228
Slettebak, A. 1951, ApJ, 113, 436
Slettebak, A. 1982, ApJS, 50, 55
Slettebak, A. 1985, ApJS, 59, 769
Steele, I. A., & Clark, J. S. 2001, A&A, 371, 643
Storey, P. J., & Hummer, D. G. 1995, MNRAS, 272, 41
Strittmatter, P. A., Woolf, N. J., Thompson, R. I., et al. 1977, ApJ, 216, 23